Deep-Sea Research, Vol. 33, No. 7, pp. 865–880, 1986.
Printed in Great Britain.

0198-0149/86 $3.00 + 0.00
Pergamon Journals Ltd.

New method reveals unexpected relationship between velocity and drag in the bathypelagic mysid *Gnathophausia ingens*

DAVID L. COWLES,* JAMES J. CHILDRESS* and DAVID L. GLUCK†

(*Received* 14 *August* 1985; *in revised form* 13 *January* 1986; *accepted* 16 *January* 1986)

Abstract—Drag and swimming speed were measured for the bathypelagic mysid *Gnathophausia ingens*, using a swim tunnel and a new design of high-resolution transducer. The crustaceans were attached to a finely balanced needle, which allowed thrust and drag forces to be detected by a sensitive tilt transducer. The tunnel was used to measure swimming speed and the relationship between velocity and drag on bodies of *G. ingens* for sizes ranging from 6 to 12 cm total length and speeds from 0 to 15 cm s^{-1}. Live mysids swam at a mean speed of 4.76 cm s^{-1}, with a pleopod beat rate of 187 beats per minute. Total drag coefficients ranged from 0.03 to 0.17. Drag on the bodies of dead mysids increased linearly with water velocity, a relationship not predicted by standard hydrodynamic equations. This linear increase is due to the change in the angle of the negatively buoyant mysid's body to the oncoming current with increasing speed. Such a linear relationship between velocity and drag would markedly increase the cost of locomotion in this mysid at low speeds, compared to that of a neutrally buoyant organism.

INTRODUCTION

AMONG the many variables affecting the rate of energy usage in pelagic organisms, locomotion is one having large energy requirements (BRETT, 1964, 1965; RAU, 1968; WEBB, 1971). The dense aquatic medium resists movements of an organism through it, giving rise to drag forces retarding the organism's motion (GORDON, 1982). Overcoming drag can raise an organism's metabolic rate by 10 times or more (BRETT, 1964; FRY, 1971; BRETT and GLASS, 1973).

Although the importance of drag on aquatic organisms has long been known, quantifying the amount of drag actually experienced by an organism while swimming has proven difficult. Mathematical formulas for predicting drag exist for only a few simple shapes under restricted conditions, few of which actually apply to many aquatic organisms (WEBB, 1975). Drag on aquatic organisms has often been estimated empirically by measuring drag on a model (STEPANOV and SVETLICHNYI, 1975) or on a dead or anesthetized organism (WEBB, 1975; BILL and HERRNKIND, 1976; SPAARGAREN, 1979) with the assumption that the living oganisms experience similar drag under similar conditions. However, these methods inadequately simulate drag around fish swimming in the common subcarangiform mode (WEBB, 1975), apparently due to the complex currents around the body during the undulations of swimming, and to extra drag produced by fin flutter in dead or anesthetized fish.

* Marine Science Institute, University of California, Santa Barbara, CA 93106, U.S.A.
† 939 Camino Del Sur, Isla Vista, CA 93117, U.S.A.

The crustacean body presents a different set of challenges in measuring drag. Crustacean bodies are bound by a relatively rigid exoskeleton, and swimming involves oscillations of protruding appendages. The fact that the body is rigid should make it easier to estimate drag using models or dead organisms. The complex shapes and often diminutive sizes of many crustaceans, however, make determination of their drag difficult to measure. Few studies of drag and swimming in crustaceans have utilized models or dead organisms. Instead, drag has been estimated from measurements of deceleration between swimming strokes (VLYMEN, 1970), or drag has been assumed to be the same as that for a simple geometric figure under similar conditions (KLYASHTORIN and YARZHOMBEK, 1973; HAURY and WEIHS, 1976; SVETLICHNYI *et al.*, 1977).

This paper presents a method for measuring drag and swimming speed directly on medium to large pelagic crustaceans, and presents such data for the bathypelagic mysid *Gnathophausia ingens*.

MATERIALS AND METHODS

Drag and swimming speeds were determined in a recirculating swim tunnel. The working section of the tunnel was a tube 5.08 cm in diameter and 51.5 cm long. Water was pumped into the upstream end of this tube through a 1.9 cm diameter plastic pipe by a centrifugal pump. The first 22 cm of the tube was a flow collimator made of clear PVC pipe. The collimator consisted of a 10 cm chamber in which the turbulence of the incoming water was dampened, and a 12 cm section packed longitudinally with plastic soda straws bounded on the upstream and downstream ends by nytex screens. These straws acted as collimators to the water stream, strongly damping large-scale turbulence (VOGEL, 1891).

The swim chamber followed the flow collimator in the working section (Fig. 1A). The chamber was made from a block of clear acrylic plastic 25.5 cm long, through which a 5.08 cm diameter hole was bored. The upstream and downstream ends of the chamber were milled round at 6.35 cm o.d. and an O-ring fitted so that the swim chamber could be easily attached to the rest of the tube using clear PVC pipe slip couplings. An acrylic lid, precision milled to fit the interior contours of the tube, was sealed by an O-ring into a slot 12.5 cm long and 3.5 cm wide cut in the roof of the swim chamber. This arrangement gave ready access to the tunnel from above for inserting and removing animals and purging bubbles, and did not distort the flow pattern through the chamber.

The transducer chamber was of clear acrylic, 11.5 cm long, 7.5 cm wide, and 5 cm high. It was centered under a slot cut through the swim chamber bottom, fastened to the swim chamber bottom by stainless steel screws, and sealed to the chamber by an O-ring. The center of the transducer chamber, under the swim chamber slot, was a well 6.5 cm long, 4 cm wide, and 3.5 cm deep. The torsion needle was mounted on a fulcrum in this chamber directly below the swim chamber slot (Figs 1B and C). The needle was a 0.78 mm diameter stainless steel wire projecting 4 cm into the swim chamber above. A small mysid-mounting hook was welded to the needle 0.32 cm above the center point of the swim chamber, in such a way that the hook was directly downstream of the needle.

The needle fulcrum was an acrylic rod mounted transverse to the direction of water flow and 1 mm below the bottom of the swim tunnel. The rod pivoted on a fulcrum of stainless steel wires inserted into supports in the chamber walls. This fulcrum allowed

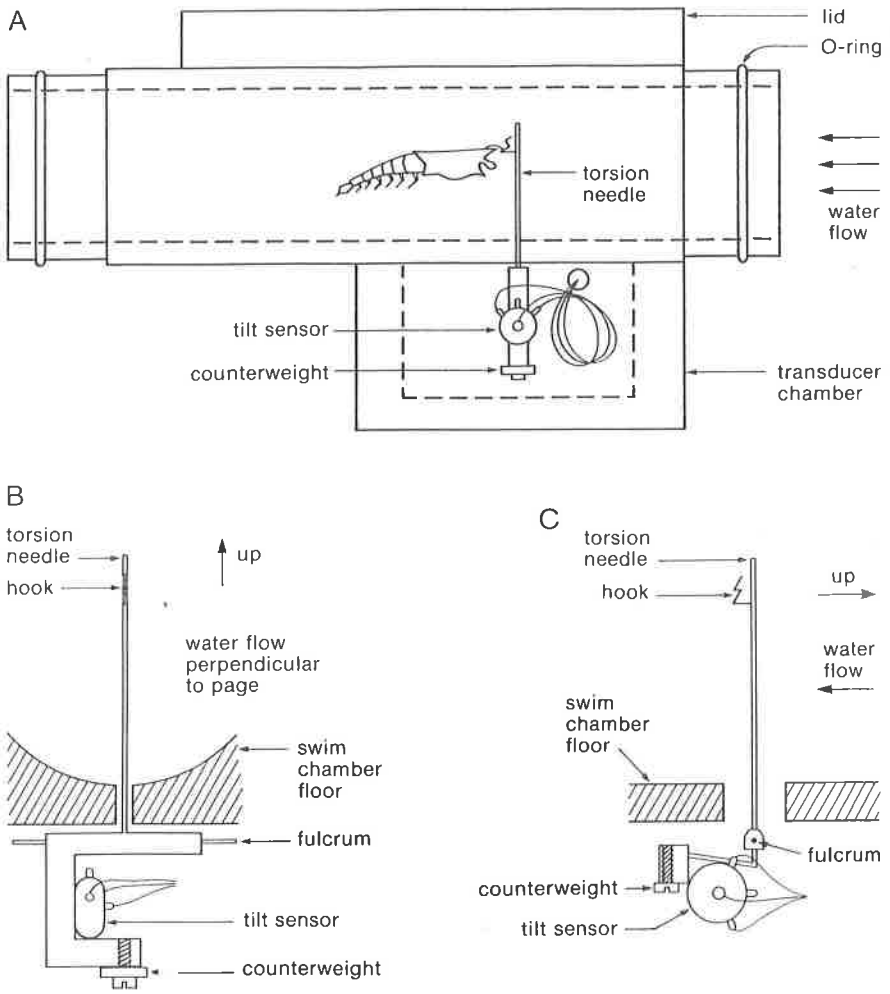

Fig. 1. (A) Swim chamber used to measure swimming speed and drag in pelagic mysids. Mysid was tethered to hook by a small stainless steel loop glued to its rostrum. (B) Torsion needle configuration for horizontal mode, chamber cross-sectional view. (C) Torsion needle configuration for the vertical chamber mode, chamber longitudinal view.

free forward and backward tilting of the torsion needle with very little friction, while preventing side-to-side motion.

Mounted below the fulcrum were the counterbalance and transducer. In the configuration for the horizontal swim chamber position (Fig. 1B), one side of the acrylic fulcrum extended below the torsion arm in a 'J' shape. In the lower portion of this 'J', directly below the torsion arm, was a threaded hole for a small stainless steel screw. This screw, along with one or more small nuts which could be attached to it, served as the counterweight, which kept the torsion needle upright when no net thrust or drag force was on the needle. The screw could be moved closer or farther from the fulcrum, or nuts could be added or removed to obtain an acceptable counterbalance. A counterweight of 1.5 g and centered 2 cm below the fulcrum was approximately correct.

Attached to the lower arm of the conterbalance 'J' was the transducer, a Spectron L-211u tilt sensor (Spectron Inc., 436 Jerusalem Ave, Uniondale, NY 11553). This sensor was a 1 cm diameter glass disk with three wire leads. If a low AC voltage was supplied to the sensor, the sensor produced a DC voltage which varied according to the angle at which the sensor was tilted. Output voltage changed by up to an order of magnitude with

a 60° tilt in either direction. Repeatability was claimed by Spectron to be within 2 arc-min. The sensor was mounted upright, with its tilt axis aligned with the tilt axis of the torsion needle so that it responded to very slight deviations of the torsion needle from vertical. To increase lead wire flexibility and minimize resistance to tilt due to lead wire stiffness, the stock lead wires were replaced with flexible 38 ga 16 strand PVC insulated wire from Cooner Wire Co. (9186 Independence Ave, Chatsworth, CA 91311). The leads were arranged in a wide loop in the transducer well, then exited through a waterproof seal in the well wall. The loop in the wire further reduced wire resistance to tilt since tilt in the sensor was translated to slight coiling and uncoiling of the loop, spreading wire flexure over a long section of the wire.

The transducer configuration for vertical swim chamber orientation (Fig. 1C) was similar to the horizontal configuration except that the torsion needle was bent at a right angle just below the fulcrum and continued parallel to the swim chamber bottom for 2 cm. The counterweight and transducer were attached to a small acrylic block fastened to the end of the needle. The tilt transducer was mounted on the block so that the transducer was upright when the swim chamber was vertical and the torsion needle was horizontal.

In use, an animal was attached to the hook on the torsion needle by a tiny loop attached to its rostrum with dental cement. The swim chamber was sealed and water pumped through the chamber. The needle held the animal's rostrum oriented into the current. If the animal swam faster or slower than the oncoming water, it tilted the torsion needle forward or back. This tilt was detected by the tilt sensor and recorded on a strip-chart or voltmeter.

Downstream from the swim chamber was another 18 cm section of clear 5.08 cm diameter PVC tube. The tube then narrowed to 2.54 cm and emptied into a chilled seawater bath. A 1/15 hp centrifugal pump recirculated water from this bath into the upstream end of the swim tunnel. Pump speed was controlled by a hand-operated variable transformer (Staco type 2PN1010).

To calibrate the torsion needle in horizontal mode, the transducer chamber was filled with chilled, degassed seawater. Chilled seawater was then run through the assembled swim chamber for one-half hour to chill all components to their 5.5°C operating temperature. The swim chamber was then quickly drained of water, the tube connecting to the rear of the chamber was removed, and the chamber was leveled with a spirit level. A thread was attached to the hook on the torsion needle. The thread ran out the back end of the swim chamber, through a light pulley, and hung down with a hook on the other end. Fine weights were hung from this hook, and the tilt sensor output was recorded. Maximum weights causing full-scale deflection of the tilt sensor were typically <0.5 g. A calibration curve of grams output was constructed from these data. Typically the curve was linear, with a correlation coefficient of 0.97 or higher, but the Y-intercept was slightly above 0. This Y-intercept represented the weight of the thread attached to the torsion arm. The grams mass were then converted to dynes force and corrected for the weight of the thread to produce a calibration of force vs output.

Needle calibration in vertical chamber mode was similar to horizontal except that the hook and thread were hung directly out the downstream end of the vertical swim chamber without the need for a pulley. Thread weight on the torsion needle could be measured directly and included in the calibration curve.

Water flow rate was measured with a King Instrument Co. K71 ball-type flowmeter

between the pump and the upstream end of the swim tunnel working section. Water velocity in the working section was then calculated from volume flow rate and the tunnel cross-section. A further correction was needed for the increase in water velocity as it moved past the obstruction produced by the animal's body in the tunnel. This correction was calculated by the formula

$$V_b = V_t \frac{A_t}{(A_t - A_b)},$$

where V_b = water velocity past animal's body, V_t = water velocity in tunnel working section, A_t and A_b = the cross-sectional areas of the tunnel and of the animal's body.

Mysid drag measurements were made in both horizontal and vertical chamber modes using the bodies of dead mysids. A fine stainless steel wire loop was glued with dental cement to the rostrum, projecting 1/2 cm in front. The thoracopods were glued to the ventral thorax because they hinge forward, and in the dead, relaxed condition they unfolded into the extended position when exposed to a water current, greatly increasing drag. The pleopods hinge backwards and it was not necessary to glue them. The dead mysid was placed in the tunnel, taking care to purge any bubbles from the gill chamber. The mysid's rostral loop was attached to the torsion needle hook, and the chamber was sealed and purged of air bubbles. Water velocity was cycled slowly between 0 and 15 cm s^{-1}, and the tiltmeter output at specific intermediate water velocities was recorded over several cycles. These measurements were then converted to dynes drag at different water velocities using the calibration curve. At the lowest velocities in the horizontal mode most mysids hung down far enough from the needle to touch the bottom of the chamber. No data for a particular water velocity were used unless the mysid was completely free of the bottom and sides at that velocity. As water velocity increased, the mysid's body assumed an increasingly horizontal orientation. This change in body angle with increasing velocity was recorded for several animals.

Torsion needle drag was determined in a similar manner to animal drag by cycling water velocity with no animal in the tunnel and recording tiltmeter output. Needle drag was very low and increased as a power of water velocity ($Y = 0.000486\ X^{1.70}$, X = cm s^{-1}, Y = dynes; $n = 15$, $R^2 = 0.98$). Drag due to the torsion needle was subtracted from all measured drag values.

To test the swim chamber for accuracy of the drag data obtained, drag was measured on a 1.27 cm diameter acrylic sphere and compared to minimum theoretical drag values calculated from hydrodynamic drag formulas for a sphere (White, 1974; Batchelor, 1967).

If an object in a flow tunnel has a cross-section which is large in relation to the size of the tunnel, extra 'horizontal drag' can be produced due to the 'blocking effect' (Webb, 1975). To reduce this effect, the animal should have a cross-section <10% of the tunnel cross-section (Bell and Terhune, 1970). *G. ingens*' body tapers gradually, with the widest point occurring in its carapace, which has a cross-section shaped like a slightly rounded isosceles triangle. The widest section of the carapace is slightly anterior to the highest section. Cross-section was estimated based on a triangle having a base equal to the greatest carapace width and an altitude equal to the greatest carapace height. No mysid was used if its cross-section calculated in this manner exceeded 10% of the chamber cross-section.

Measurements of spontaneous swimming speed were made similarly to the drag measurements, using the horizontal chamber mode. A hook was glued to the rostrum of a live mysid, which was placed in the chamber. Water was pumped through the tunnel at an intermediate velocity for $\frac{1}{2}$ to 1 h to allow the mysid to become accustomed to chamber conditions. Water speed was then altered until the tiltmeter output indicated no net force on the torsion needle. Under these conditions the mysid's forward swimming speed was equal to the water's velocity. The water flow rate, corrected for the increase in water velocity around the mysid caused by the narrowing of the tunnel effective cross-section as the water was forced to move around the mysid's body, was recorded as the mysid's swimming speed. The mysid was allowed to continue swimming for a number of hours, with a new measurement of swimming speed being made several times per hour.

During swimming speed measurements, pleopod beat rate was periodically measured visually using a stopwatch, and was recorded along with swimming speed.

Linear regressions were calculated on all drag data, and the best fit equation from the equations $Y = a + bX$, $Y = ae^{bX}$, $Y = aX^b$, and $Y = a + b\ \ln(X)$ was selected (Y = drag, X = velocity). Similar regressions were calculated for change in body angle with velocity in selected animals, for carapace length vs total length, body height, body width, and calculated body cross-section, and for these body dimensions vs the slope and Y-intercepts in the velocity-drag equations. In addition, a t-test was used to compare drag coefficients and Y-intercepts in the velocity-drag equations between small individuals (carapace length <3.2 cm, total length <9 cm) and those larger than this size.

Measured drag of the sphere and of the mysids was compared with the drag predicted by hydrodynamic formulas for a smooth hard sphere (WHITE, 1974; BATCHELOR, 1967), and for a hard fusiform shape (WEBB, 1975) having a length equal to that of the mysid, a diameter equal to the mean of the mysid's maximum carapace height and width, and a surface area equal to that of a cylinder of the same length and diameter (no ends). The drag predicted by the hydrodynamic formulas was assumed to be the theoretical minimum drag the sphere or mysid would experience under ideal conditions.

In the live, swimming mysids, variations in swimming velocity and the restricted size range of organisms for which data was obtainable during the experiment prevented calculation of reliable regressions of swimming speeds and pleopod beat rates; therefore these data were merely tabulated in summary form with means and standard deviations for each organism.

RESULTS

Drag values measured on the sphere increased exponentially with speed, as predicted by hydrodynamic equations, but were approximately 10% higher than the values predicted for ideal conditions (Fig. 2).

The animal usually oriented steadily into the current during the experiment. A few live mysids oscillated in the current, swam unsteadily, and performed occasional tail-flips. It was found that moving their rostral loop from its position directly ahead of the anterior point of the rostrum to one slightly ventral to this position eliminated the body oscillations and improved the mysid's swimming steadiness. With some dead mysids the tiltmeter output was unsteady, indicating turbulence around the body. This usually resulted from a leg projecting at an awkward angle. Securing the leg to the body generally eliminated these oscillations. Flow around several of the dead mysids con-

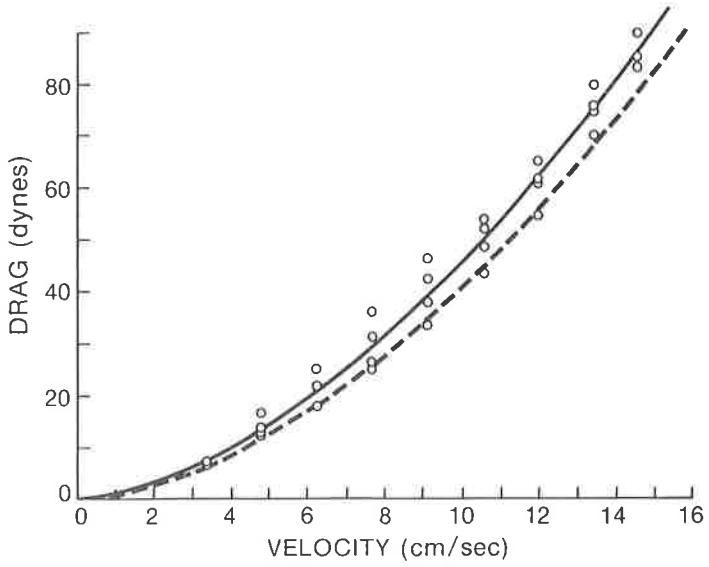

Fig. 2. Drag on a sphere. Plotted points are measured data. Solid line is the best-fit regression of measured data $Y = 0.954\ X^{1.68}$, $n = 33$, $R^2 = 0.98$. Dashed line is the minimum theoretical drag on a sphere based on hydrodynamic drag formula $Y = 0.771\ X^{1.725}$.

tinued turbulent even though no irregular body projections were noted. It is possible that this turbulence was due to unequal angles of projection of the antennal scales. Data from these mysids were not used.

Gnathophausia ingens is more dense than seawater (CHILDRESS and NYGAARD, 1974). In both the live swimming and dead drag measurements, the animal hung down at an angle from the needle at 0 water velocity. As velocity increased, its body assumed an increasingly horizontal position (Fig. 3).

Drag was measured on the bodies of 29 mysids in the horizontal mode and on 21 in the vertical mode. Replicates of drag values for a particular animal at a particular water velocity varied by 3–10 dynes (1–3% of maximum drag values measured), depending on chamber configuration. The relationship between velocity and drag in the horizontal mode was linear, with a correlation coefficient of 0.95 or higher (Fig. 3). In 24 of the 29 horizontal cases, drag at the highest speed measured (approximately 15 cm s^{-1}) was higher than the drag predicted by a regression from the lower speeds. In 11 of these cases, measured drag was significantly higher than predicted ($P < 0.05$).

The Y-intercept of the best-fit regression curve in both horizontal and vertical modes was greater than zero. Since the drag of a non-moving body by definition is zero, a mysid was modified to determine the source of the indicated drag at zero velocity (Fig. 4). Drag was first measured in the normal manner in the horizontal mode (Fig. 4, solid line). A 0.25 g weight was then tucked into the mysid's gill chamber to change its dead weight and density but no other parameter. The relationship between velocity and drag, represented by the line's slope, was not significantly different, but the Y-intercept was greatly increased (Fig. 4, dashed line). The weights were then removed and all the mysid's legs cut off to produce a smoother body surface. The drag then increased more slowly with increasing water velocity (Fig. 4, dash-dotted line). From these data we concluded that the line slope is determined by increase in drag with increasing velocity, while the nonzero Y-intercept is due to the dead weight of the mysid, which remains the same at all swimming speeds.

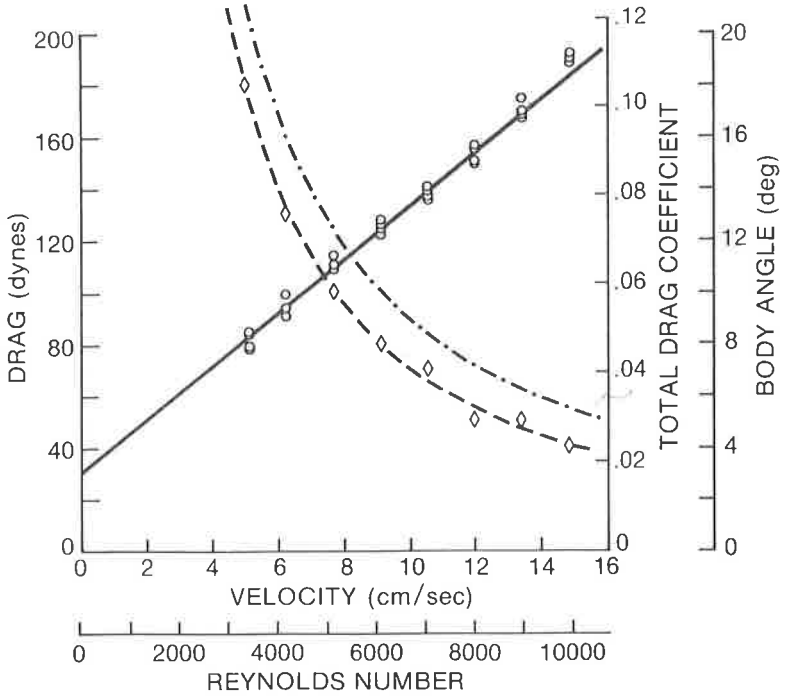

Fig. 3. Solid line and circles: a typical velocity (cm s^{-1}) vs drag (dynes) relationship for the body of *G. ingens*, using the horizontal chamber mode. Carapace length of this individual was 3.52 cm. Regression line: $Y = 28.38 + [illegible]X$, $n = 32$, $R^2 = 0.99$. Dash-dotted line: total drag coefficient ($C_{d\ tot}$) vs Reynolds number. Regression line: $Y = 2837.8\ X^{-1.24}$, $n = 32$, $R^2 = 0.99$. Dashed line and diamonds: change in body angle from horizontal (deg) vs velocity (cm s^{-1}). Regression line: $Y = 154.14\ X^{-1.345}$, $n = 8$, $R^2 = 0.99$.

Correction for the above regression: Y = 28.38 + 10.64X DLC

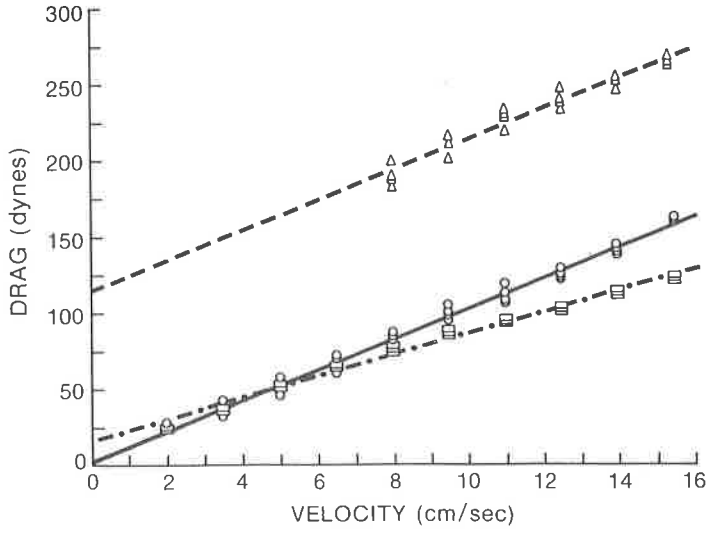

Fig. 4. Measurements of drag on a mysid body of 2.75 cm carapace length, using the horizontal chamber mode. Solid line and plotted circles was an unmodified mysid ($Y = 2.74 + 10.03\ X$, $R^2 = 0.99$). Dashed line and plotted triangles was for the same mysid with an extra 0.25 g weight tucked into its branchial chamber ($Y = 115 + 9.97\ X$, $R^2 = 0.96$). Dash-dotted line and plotted squares was for mysid with no weights and with legs removed ($Y = 16.3 + 7.06\ X$, $R^2 = 0.99$).

The measured drag force on an animal's body in the horizontal mode was divided into two components; the Y-intercept, due to the constant dead weight of the animal, and the slope, due to the increase in drag with increasing speed. The rate of increase (Y) in drag with increasing speed was most closely related to the mysid's cross-sectional area (X) ($Y = 9.0\ X - 0.63$, $R^2 = 0.801$) and to total length (X) ($Y = 0.042\ X^{2.46}$, $R^2 = 0.870$). Table 1 contains regression equations for conversions between body dimensions. Carapace length was selected as the standard size measurement rather than total length or cross-sectional areas because carapace length is quickly and directly measurable and does not change with changes in the mysid's position. The best-fit regression between velocity (Y) and increase in drag (Z) with speed in the horizontal mode was calculated for the entire range of carapace lengths (X) of mysids studied. The best-fit regression was $Z = Y \times 0.862\ X^{2.048}$; $n = 27$, $R^2 = 0.88$. The range of carapace lengths to which this regression applies was 2.0–4.3 cm, which corresponds to total lengths of 6.15–11.61 cm. Velocities used in the regression were from 3 to 15 cm s^{-1}.

The correlation between carapace length (X) and Y-intercept (Y) of the measured drag relationship was lower than the correlation between carapace length and increase in drag with increase in speed, due to variability in the Y-intercepts. This variability presumably resulted from differences in mysid density at different stages of the molt cycle and in different nutritional states. The best-fit regression was $Y = 6.358\ X^{1.315}$; $n = 24$, $R^2 = 0.22$. In spite of this low correlation, a t-test indicated a highly significant difference ($P < 0.01$) between the Y-intercepts of animals having a carapace length <3.2 cm (total length <9.0 cm, mean Y-intercept = 22.74) and those with carapace length of 3.2 cm or longer (mean Y-intercept = 43.60).

In the vertical mode, there was a power relationship between velocity and drag, with a correlation coefficient of 0.95 or higher (Fig. 5).

Total drag coefficients ($C_{d\ \mathrm{tot}}$) for the horizontal mode were calculated based on the measured drag data. Calculations of total drag coefficients for the vertical mode were based on measured drag values minus the animal's dead weight in water (the Y-intercept of the measured drag data in Fig. 5). Table 2 contains the best-fit regressions between total length (X) and $C_{d\ \mathrm{tot}}$ (Y) for a range of speeds in both horizontal and vertical modes. A t-test at each speed indicated that total drag coefficient was slightly higher for mysids having a carapace length ≥3.2 cm (total length >9.0 cm) than for individuals smaller than this size. Change in $C_{d\ \mathrm{tot}}$ with speed is shown in Fig. 3 for the horizontal mode and in Fig. 5 for the vertical mode.

In the live swimming experiments, only a small size range of mysids could be used. For very small mysids, with a carapace length of <1.7 cm, it was difficult to glue a small

Table 1. *Regressions for interconverting size measurements in* G. ingens*

X	Y	Equation	n	R^2	Range of X
Carapace length (cm)	Cross-section (cm^2)†	$Y = 0.113\ X^{1.983}$	51	0.99	1.5– 4.4
Carapace length (cm)	Carapace width (cm)	$Y = 0.038 + 0.479\ X$	51	0.96	1.5– 4.4
Carapace length (cm)	Carapace height (cm)	$Y = -0.007 + 0.452\ X$	51	0.98	1.5– 4.4
Carapace length (mm)	Total length (mm)	$Y = 14.04 + 2.37\ X$	69	0.99	1.7– 4.4
Wet weight (g)	Carapace length (cm)	$Y = 18.56\ X^{0.350}$	135	0.99	0.1–38.1

* For further regressions see CHILDRESS and PRICE (1983).

† The carapace was triangular in cross-section. Cross-section was estimated as the area of a triangle with altitude equal to the greatest carapace height and base equal to greatest carapace width.

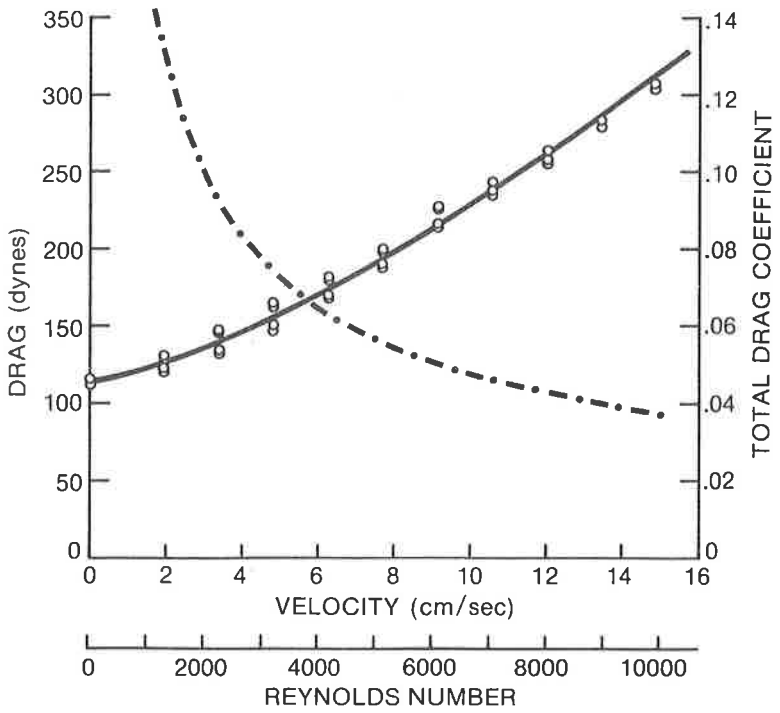

Fig. 5. Measurements of drag on a mysid body using the vertical chamber mode. Mysid was the same as in Fig. 3. Solid line and plotted circles: velocity (cm s^{-1}) vs drag (dynes). Regression: $Y = 4.75\ X^{1.42} + 124$, $n = 39$, $R^2 = 0.98$. Dashed-dotted line: total drag coefficient ($C_{d\ tot}$) vs Reynolds number. Regression: $Y = 9.985\ X^{-0.609}$, $n = 39$, $R^2 = 0.86$.

Table 2. Total drag coefficients on G. ingens *in the horizontal and vertical modes:* *X = *total length* (cm); Y = *total drag coefficient at the given Reynolds number*

Mode	Reynolds number	Regression	R^2	n
Horizontal	1000	$Y = -0152 + 0.313\ 1n\ X$	0.063	29
Horizontal	3000	$Y = -0.113 + 0.113\ 1n\ X$	0.247	29
Horizontal	5000	$Y = 0.007\ X^{1.05}$	0.521	29
Horizontal	10,000	$Y = 0.00186\ X^{1.273}$	0.704	29
Vertical	1000	$Y = 0.0314\ X^{0.686}$	0.463	20
Vertical	3000	$Y = 0.0187\ X^{0.635}$	0.489	20
Vertical	5000	$Y = 0.0152\ X^{0.596}$	0.446	20
Vertical	10,000	$Y = 0.0112\ X^{0.556}$	0.346	20

* Measured drag values at zero velocity were subtracted from vertical mode data before calculating regressions.

enough hook to their rostrum so that their density and swimming trim were not adversely affected. On the other hand, animals over 2.6 cm carapace length swam steadily in the chamber at first, but soon stretched out their thoracopods and touched the wall. Once they detected the wall or floor of the tunnel, they would swim for a brief period, then reach out for the wall, greatly increasing their drag, changing their swimming speed, and making it impossible to measure a steady rate of swimming. Measurements of free-swimming speeds were obtained for only a few of these larger mysids, and even then only for brief periods of swimming.

Mean swimming speed in the live mysids was 4.76 cm s^{-1} (0.52 lengths s^{-1}), slightly slower than the 5.6 cm s^{-1} routine speeds reported by KILS (1979) for *Euphausia superba*

Table 3. Size, swimming speeds, and pleopod beat rates of 13 G. ingens

Carapace length (cm)	Total length (cm)	Swimming speed (cm s^{-1}) Mean	S.D.	Pleopod beats per minute Mean	S.D.	*n*
3.57	9.88	8.8	–	187	–	1
3.01	8.55	10.3	–	138	–	1
2.20	6.63	3.97	0.356	182	9.90	18
2.57	7.50	3.57	0.388	170	4.56	6
1.89	5.89	1.35	0.10	206	3.42	4
2.72	7.86	3.00	0.122	202	4.77	5
2.29	6.84	3.12	0.05	151	8.26	4
2.08	6.34	3.50	0.0	174	0.0	2
1.97	6.08	5.87	0.796	190	8.76	25
2.01	6.18	5.98	0.233	194	4.82	9
1.99	6.13	4.14	0.279	203	4.00	22
1.94	6.01	4.47	0.480	198	8.78	9
1.85	5.80	5.60	0.348	189	3.40	28

of 40–50 mm length. Mean pleopod beat rate was 187 beats min^{-1} (Table 3), which is within the range of routine pleopod beat rates reported by QUETIN and CHILDRESS (1980) for *G. ingens*.

DISCUSSION

The empirically measured linear relationship between velocity and drag in these mysids is unusual. Theoretical drag formulas (BATCHELOR, 1967) predict that drag should be proportional to a power of the velocity, and previous measurements on the drag of fish (e.g. WEBB, 1971; MAGNUSON, 1978) have generally yielded a power relationship. Many papers estimating theoretical drag on fish and crustaceans (e.g. VLYMEN, 1970; KLYASHTORIN and YARZHOMBEK, 1973; HAURY and WEIHS, 1976; SVETLICHNYI *et al.*, 1977; KLYASHTORIN, 1978) have been based on these theoretical formulas.

The fact that *G. ingens'* density is greater than that of seawater caused the angle of orientation of the animal's body to change with changes in water velocity. At slow speeds the animal hung down at an angle, while as the speed increased the body assumed an orientation increasingly parallel to the current. To determine whether the empirically measured linear relationship was due to this change in the mysid's body angle with change in water flow velocity, the swim chamber was oriented vertically, with the dead mysid facing directly up into the downflowing current. In this orientation gravitational force was parallel to drag force, so the vector sum of both forces was always directly downstream and the mysid's body was always oriented parallel to the water current. Under these conditions, drag increased as a power of speed, as predicted by hydrodynamic equations. From these results we conclude that the change in attitude with speed in these mysids produced the linear relationship between velocity and drag. Simple hydrodynamic drag theory does not apply to these mysids since the theory assumes that the object is always oriented directly into the current. NACHTIGALL and BILO (1975) have shown that the drag of dytiscid beetles greatly increases with an increase in body angle to the oncoming water. It was apparently this increase in drag with increased body angle at low velocities which produced the linear speed-drag relationship in the horizontal mode.

Of the two modes used to measure drag—horizontal and vertical—the horizontal mode most nearly simulates conditions experienced by free-swimming mysids. We thus postulate that *G. ingens* experiences a linearly changing drag relationship with velocity while swimming under natural conditions in the ocean.

The measured drag values obtained in this experiment represent two forces which the swimming mysid must overcome to swim horizontally through the water. In an aquatic organism swimming at constant velocity, useful thrust is used both to produce lift, if needed, and to overcome drag (HARGREAVES, 1981). Thus the negatively buoyant *G. ingens* must not only overcome drag to move forward, but, because of its negative buoyancy, also must constantly compensate for the downward force of gravity. This accounts for the nonzero *Y*-intercepts in the measured drag values. If *G. ingens* were neutrally buoyant, it would not need to counteract gravitational force. Swimming thrust could be used to propel the body directly forward instead of upward and forward. Its body would thus not change angles with changes in speed, and its drag relationship would be similar to that measured in the vertical mode. Furthermore, the *Y*-intercept can be subtracted from the drag measurements in the vertical mode (Fig. 6). This new relationship predicts what the velocity–drag relationship would be for *G. ingens* if the mysid were neutrally buoyant. Except at the highest speeds, drag experienced by a neutrally buoyant mysid (represented by the vertical mode data minus *Y*-intercept values) would be lower than the values measured in the horizontal mode. The greatest differences between the two occur at lower speeds. At all speeds, the drag predicted for a neutrally buoyant mysid would be 2–2.5 times higher than that of a smooth fusiform body as predicted by hydrodynamic equations, while the actual drag as measured in the horizontal mode is even higher (Fig. 6).

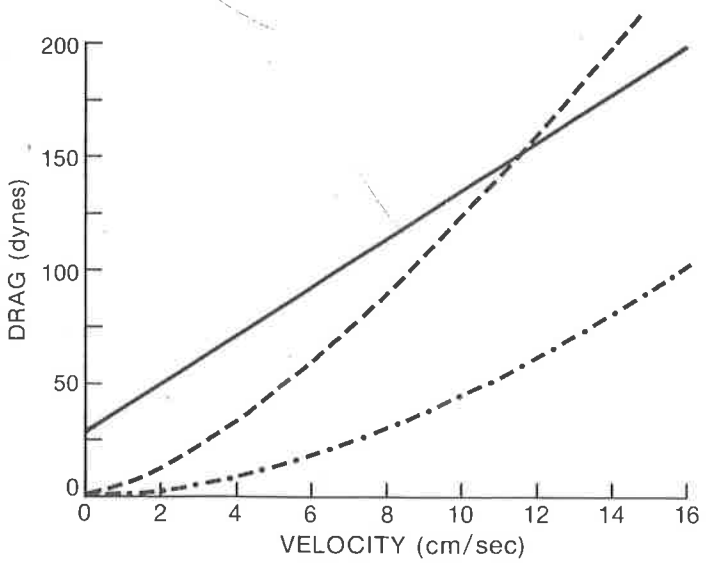

Fig. 6. Relationship between velocity and drag for a mysid body of 3.53 cm carapace length, measured in the horizontal mode (solid line) and in the vertical mode minus *Y*-intercept values (dashed line). Vertical mode line represents the drag this mysid would experience if it were neutrally buoyant. Dash-dotted line is the calculated minimum theoretical drag on this mysid, using hydrodynamic drag formulas for a smooth, spindle-shaped body having the same length and cross-section as the mysid. Horizontal drag regression: $Y = 28.38 + 10.6\,X$. Vertical drag regression: $Y = 4.75\,X^{1.42}$. Minimum theoretical drag line: $Y = 0.778\,X^{1.76}$.

The large difference in drag at low speeds between values measured for these mysids in the horizontal mode and the drag they would experience if neutrally buoyant, as estimated by the vertical mode, suggests that these animals have a high cost of transport at low speeds, as compared to neutrally buoyant animals. This trend is also indicated by the high drag coefficients calculated for the mysid at low speeds in the horizontal mode. *G. ingens*' ability to conserve energy by swimming slowly can thus be expected to be limited by the animal's high cost of transport at low speeds.

In living mysids, other factors related to the change in attitude with speed may further increase the drag coefficient at low speeds. *G. ingens* is an active crustacean, and pumps water rapidly through its branchial chamber. Water leaving the branchial chamber is ejected forcefully in a direction ventral to the mysid's carapace. At low speeds, the higher angle of the mysid's body to the water would cause a larger vector component of momentum of this exhaled water to be directed forward, producing resistance to forward movement. The extent to which this effect might increase the drag on live swimming mysids over drag on dead mysids has not been quantified.

The effect of the torsion needle directly upstream from the mysid on drag and flow characteristics around the body was also not quantified. However, this effect is likely to be very small. DUBOIS and OGILVY (1978) and OGILVY and DUBOIS (1981) found that an entire screen just upstream from a swimming fish had only a slight effect on turbulence around the fish, and that drag was not significantly increased even when a spinning paddle was placed upstream to increase turbulence greatly. SEELEY *et al.* (1975) found that a 3.175 mm diameter rod used to support a 3.495 and a 6.08 cm diameter sphere in a flow chamber had very little effect on flow patterns over the spheres, even directly downstream from the rod, at Reynolds numbers for the spheres of from 750 to 3000. Calculations from equations given by VOGEL (1981) indicate that the diameter of the torsion needle was below the critical diameter for surface roughness required to significantly affect flow and turbulence in a pipe at the flow velocities used.

At high water velocities, the mysid's body assumed an angle nearly parallel with the current. Under these conditions drag on the body in the horizontal mode can be expected to be similar to drag measured in the vertical mode, since in the vertical mode the mysids' bodies also remained parallel to the current. At these high water velocities, the drag would begin to increase with a power of the water velocity, as predicted by hydrodynamic equations and as measured in vertical mode, rather than increasing linearly with water velocity as it did at lower speeds in the horizontal mode. This prediction is supported by the fact that most horizontal drag values measured at the highest water velocities (13–15 cm s^{-1}) were higher than that predicted from a linear regression on lower speeds, and were intermediate between these predicted values and the higher values predicted by a power regression of the vertical drag data (Figs 3 and 6). However, no mysid was observed to swim routinely at the rates at which this change occurred, so it is unclear whether they routinely encounter these conditions in life.

Although this linear relationship between velocity and drag is unusual, it is not unique. MAYHEAD (1973) found a linear relationship between wind velocity and drag on conifers. He attributed this relationship to changes in the needle and branch orientation with increasing wind. The data of OGILVY and DUBOIS (1981) show a linear relationship between drag and velocity in bluefish, and that the relationship changes with buoyancy. Tail thrust calculations (OGILVY and DUBOIS, 1982) also support this relationship. Tail thrust can be used to estimate drag because in steady swimming, thrust equals drag

(NEWMAN and WU, 1975). It is possible, however, that changes in parameters other than body orientation, such as pectoral fin position, could have produced this linear thrust–drag relationship.

IVLEV (1963) measured metabolic cost of swimming, as measured by oxygen consumption, in the shrimp *Palaemon squilla*. He reported that metabolic cost of swimming increased as a power of velocity, as predicted by hydrodynamic drag equations. However, he noted that at the lowest swimming speeds measured, 0.61 cm s^{-1}, metabolic rate was higher than that predicted by a power regression on the rest of the speeds. He assumed that this higher metabolic cost was due to additional unnecessary movements of the shrimp at these low speeds. However, an elevated metabolic cost at low speeds could also be explained by increases in the animal's body angle to the oncoming current at these speeds, as in *G. ingens*. Ivlev did not report whether *P. squilla* changed body angles at low velocities, however; HARGREAVES (1981) shows drawings of another crustacean, *Neomysis americana*, of generally similar size and body shape, swimming into a 1–3 cm s^{-1} current. The mysid's body is clearly at an angle to the oncoming current. Hargreaves speculates that this inclined angle may be used to generate lift at low swimming speeds.

A linear relationship between swimming speed and drag would be expected to apply only to a restricted class of organisms, if the relationship is produced by changing angles of attack to the water as in *G. ingens*. It would not be expected to apply to organisms such as neutrally buoyant fish, since they can maintain the same angle of attack at any speed, nor to very small crustaceans, which swim at very low Reynolds numbers (NACHTIGALL, 1981). At low Reynolds numbers drag is due primarily to viscous effects, and changes in body shape and orientation have little effect on drag (STRICKLER, 1975). The linear relationship may apply to any organism which swims at intermediate or high Reynolds numbers, has a rigid exterior, and is negatively bouyant. Among other pelagic crustaceans, euphausiids and sergestid shrimp also match these characteristics (CHILDRESS and NYGAARD, 1974), and thus may also experience a linear relationship between velocity and drag. This may at least partially account for the high cost of transport found for *Euphausia pacifica* (TORRES, 1984). Torres calculated metabolic power consumption based on oxygen consumption of swimming euphausiids, and compared this to the power required to overcome the animal's theoretical drag based on hydrodynamic equations. He found a high metabolic cost as compared to the theoretical power of transport, and concluded that *E. pacifica* swims with low efficiency. He states that one possible source of error in his calculations is that theoretical drag, as calculated from hydrodynamic equations, may be lower than drag actually experienced by the euphausiid. As this paper has shown, actual drag may indeed be higher than that calculated by hydrodynamic equations for such an organism, especially at low speeds. This conclusion is further supported by the fact that *E. pacifica* was found to have a linear relationship between oxygen consumption and swimming speed (TORRES and CHILDRESS, 1983), which is consistent with the drag data reported in this paper. *E. pacifica* thus may be experiencing higher drag and cost of transport than calculated by TORRES (1984).

Acknowledgements—We wish to thank G. Beitzer of Spectron Inc., and H. Stuber, C. Beehler, and S. Kaiser for their parts in building swim chamber and transducer components. Our thanks also to M. S. Gordon, G. T. Yates, A. Alldredge, A. Ebeling, N. Sanders, J. Favuzzi, A. Anderson, and an anonymous reviewer for their helpful criticisms of earlier drafts of this paper. This research was supported by NSF grants OCE78-08933, OCE81-10154, and OCE85-00237 to Dr J. J. Childress.

REFERENCES

BATCHELOR G. K. (1967) *An introduction to fluid dynamics.* Cambridge Univeristy Press, 634 pp.

BELL W. H. and L. D. B. TERHUNE (1970) Water tunnel design for fisheries research. *Fisheries Research Board of Canada Technical Report*, **195**, 69 pp.

BILL R. G. and W. F. HERRNKIND (1976) Drag reduction by formation movement in spiny lobsters. *Science*, **193**, 1146–1148.

BRETT J. R. (1964) The respiratory metabolism and swimming performance of young sockeye salmon. *Journal of the Fisheries Research Board of Canada*, **21**, 1183–1226.

BRETT J. R. and N. R. GLASS (1973) Metabolic rates and critical swimming speeds of sockeye salmon (*Oncorhynchus nerka*) in relation to size and temperature. *Journal of the Fisheries Research Board of Canada*, **30**, 379–387.

CHILDRESS J. J. and M. NYGAARD (1974) Chemical composition and buoyancy of midwater crustaceans as function of depth of occurrence off southern California. *Marine Biology*, **27**, 225–238.

CHILDRESS J. J. and M. H. PRICE (1983) Growth rate of the bathypelagic crustacean *Gnathophausia ingens* (Mysidacea: Lophogastridae) II. Accumulation of material and energy. *Marine Biology*, **76**, 165–177.

DUBOIS A. B. and C. S. OGILVY (1978) Forces on the tail surface of swimming fish: thrust, drag and acceleration in bluefish (*Pomatomus saltatrix*). *Journal of Experimental Biology*, **77**, 225–241.

FRY F. E. J. (1971) The effect of environmental factors on the physiology of fish. In: *Fish physiology*, Vol. 6, W. S. HOAR and D. J. RANDALL, editors, Academic Press, New York, pp. 1–98.

GORDON M. S. (1982) *Animal physiology: principles and adaptations*, 4th edn, Macmillan, New York, 635 pp.

HARGREAVES B. R. (1981) Energetics of crustacean swimming. In: *Locomotion and exercise of arthropods*, C. F. HERREID and C. R. FOURTNER, editors, Plenum Press, New York, pp. 453–490.

HAURY L. and D. WEIHS (1976) Energetically efficient swimming behaviour of negatively buoyant zooplankton. *Limnology and Oceanography*, **21**, 797–803.

IVLEV V. S. (1963) Energy consumption during the motion of shrimps. *Zoological Zhurnal*, **43**, 1465–1471.

KILS U. (1979) Performance of Antarctic krill *Eupausia superba* at different levels of oxygen saturation. *Meeresforschung*, **27**, 35–48.

KLYASHTORIN L. B. (1978) Estimation of energy expenditures for active swimming and vertical migrations in planktonic crustaceans. *Oceanology*, **18**, 91–94.

KLYASHTORIN L. B. and A. A. YARZHOMBEK (1973) Energy consumption in active movements of planktonic organisms. *Oceanology*, **13**, 575–580.

MAGNUSON J. (1978) Locomotion by scombrid fishes: hydromechanics, morphology, and behavior. In: *Fish physiology*, Vol. VII, W. S. HOAR and D. J. RANDALL, editors, Academic Press, New York, pp. 240–315.

MAYHEAD G. J. (1973) Some drag coefficients for British forest trees derived from wind tunnel studies. *Agricultural Meteorology*, **12**, 123–130.

NACHTIGALL W. (1981) Hydromechanics and biology. *Biophysics of Structure and Mechanism*, **8**, 1–22.

NACHTIGALL W. and D. BILO (1975) Hydromechanics of the body of *Dytiscus marginalis* (Dytiscidae, Coleoptera). In: *Swimming and flying in nature*, Vol. 2, T. Y. T. WU, C. J. BROKAW and C. BRENNEN, editors, Plenum Press, New York, pp. 585–595.

NEWMAN J. N. and T. Y. T. WU (1975) Hydromechanical aspects of fish swimming. In: *Swimming and flying in nature*, Vol. 2, T. Y. T. WU, C. J. BROKAW and C. BRENNEN, editors, Plenum Press, New York, pp. 615–634.

OGILVY C. S. and A. B. DUBOIS (1981) The hydrodynamic drag of swimming bluefish (*Pomatomus saltatrix*) in different intensities of turbulence: variation with changes of buoyancy. *Journal of Experimental Biology*, **92**, 67–85.

OGILVY C. S. and A. B. DUBOIS (1982) Tail thrust of bluefish *Pomatomus saltatrix* at different buoyancies, speeds, and swimming angles. *Journal of Experimental Biology*, **98**, 105–117.

QUETIN L. B. and J. J. CHILDRESS (1980) Observations on the swimming activity of two bathypelagic mysid species maintained at high hydrostatic pressures. *Deep-Sea Research*, **27**, 383–391.

RAU G. M. M. (1968) Oxygen consumption of rainbow trout (*Salmo gairdneri*) in relation to activity and salinity. *Canadian Journal of Zoology*, **46**, 781–786.

SEELEY L. E., R. L. HUMMEL and J. W. SMITH (1975) Experimental velocity profiles in laminar flow around spheres at intermediate Reynolds numbers. *Journal of Fluid Mechanics*, **68**, 591–608.

SPAARGAREN D. H. (1979) Hydrodynamic properties of benthic marine crustacea. I. Specific gravity and drag coefficients. *Marine Ecology Progress Series*, **1**, 351–359.

STEPANOV V. N. and L. S. SVETLICHNYI (1975) Calculation of the rate of passive vertical migration of planktonic organisms. *Oceanology*, **15**, 221–223.

STRICKLER J. R. (1975) Swimming of planktonic *Cyclops* species (Copepoda: Crustacea): pattern, movements and their control. In: *Swimming and flying in nature*, Vol. 2, T. Y. T. WU, C. J. BROKAW and C. BRENNEN, editors, Plenum Press, New York, pp. 599–613.

SVETLICHNYI L. S., Y. A. ZAGORODNYAYA and V. N. STEPANOV (1977) Bioenergetics of copepods *Pseudocalanus elongatus* during migration. *Soviet Journal of Marine Biology*, **3**, 430–436.

TORRES J. J. (1984) Relationship of oxygen consumption to swimming speed in *Euphausia pacifica*. II. Drag, efficiency and a comparison with other swimming organisms. *Marine Biology*, **78**, 231–237.

TORRES J. J. and J. J. CHILDRESS (1983) Relationship of oxygen consumption to swimming speed in *Euphausia pacifica*. I. Effects of temperature and pressure. *Marine Biology*, **74**, 79–86.

VLYMEN W. J. (1970) Energy expenditure of swimming copepods. *Limnology and Oceanography*, **15**, 348–356.

VOGEL S. (1981) *Life in moving fluids*. Princeton University Press, 352 pp.

WEBB P. W. (1971) The swimming energetics of trout. II. Oxygen consumption and swimming efficiency. *Journal of Experimental Biology*, **55**, 521–540.

WEBB P. W. (1975) Hydrodynamics and energetics of fish propulsion. *Bulletin of the Fisheries Research Board of Canada*, **90**, 159 pp.

WHITE F. M. (1974) *Viscous fluid flow*. McGraw-Hill, New York, 640 pp.